Journal of the Iranian Chemical Society (2020) 17:1059–1072
https://doi.org/10.1007/s13738-019-01833-w

ORIGINAL PAPER

Pd–ninhydrin immobilized on magnetic nanoparticles: synthesis, characterization, and application as a highly efficient and recoverable catalyst for Suzuki–Miyaura and Heck–Mizoroki C–C coupling reactions

Maryam Hajjami[1] · **Zeinab Shirvandi**[1]

Received: 24 May 2019 / Accepted: 16 December 2019 / Published online: 2 January 2020

Abstract

In this work by controlling the interaction between the inorganic complexes and the support material, we have designed a high-activity nanostructured combined of magnetic nanoparticles and Pd–ninhydrin-terminated complex as catalyst. The as-prepared catalyst was characterized by FT-IR, XRD, VSM, SEM, EDAX, ICP, and TGA techniques. This magnetic nanostructure can be used as a novel, green, and efficient heterogeneous catalyst for Suzuki–Miyaura and Heck–Mizoroki C–C coupling reactions. This catalyst showed promising catalytic activity and excellent yields toward various aryliodides and arylbromides in mild reaction conditions. In Suzuki–Miyaura reactions, various aryl halides (I, Br) were coupled with phenyl boronic acids in 5 mg of catalyst and 8 mg of catalyst used for Mizoroki–Heck reaction of aryl halides (I, Br) with *n*-butyl acrylate or acrylonitrile. The catalyst was reusable and recycled six times without a significant loss in activity and leaching of palladium.

Graphic abstract

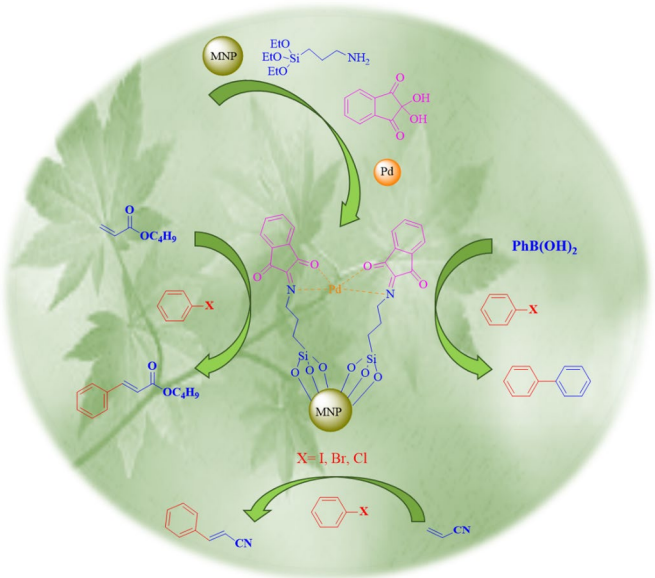

Keywords Pd–ninhydrin complex · Fe_3O_4 · Suzuki reaction · Heck reaction · C–C coupling

Extended author information available on the last page of the article

Introduction

An interesting goal in green chemistry is the development and improvement of the catalytic processes and homogeneous catalysts, which include removal of toxic and expensive reagents, minimization of by-products, and simplification of workup procedures [1]. Homogeneous catalyst has the advantage due to accessibility of all catalytic sites to reactants in solution and, possibility to tune the chemo, regio and enantio selectivity of the catalyst, high selectivity, better yield, and higher turnover numbers. Although homogeneous catalysts are very active and are widely used in a number of commercial applications, but have two main problems, time consumed for the catalyst separation from the reaction mixture and tedious recovery process. One efficient way to solve these problems in homogeneous catalysis is the heterogenization of active catalytic molecules which would be the use of a heterogeneous catalyst [2–5]. Despite the advantages of heterogeneous catalysis, such as easy separation, efficient recycling, minimization of metal traces in the product, and waste disposal, they having lower reactivity and selectivity than corresponding homogeneous catalysts. Therefore, there is need to a catalyst system that can show high activity and selectivity on one hand, and also the ease of catalyst separation and recovery on the other hand [6–8].

With the development of nanoscience and nanotechnology, chemists achieved the various catalytic reactions due to a wide variety of nanostructured catalysts or immobilization of homogeneous catalysts on nanostructured supports such as mesoporous molecular sieve (MCM-41 [9], MCM-48 [10], and SBA-15 [11]), metal organic framework materials [12] bohemite [13], polymers [14], and graphene oxide [15]. Recently, magnetic nanoparticles (MNPs) have attracted great interest due to their remarkable advantages such as small size, large specific surface area, excellent catalytic activity and selectivity, easy synthesis and functionalization, and high dispersion property as well as low toxicity and price. Moreover, the intrinsic advantage of magnetic nanoparticles is that it can be effective and easily separated from the reaction mixture by applying an external magnetic without using of tedious filtration. Thus, novel nanoparticles efficiently bridge the gap between homogeneous and heterogeneous catalysis that preserving the desirable attributes of both systems [16–21]. In recent years, there are several reports of magnetic nanocatalysts that contain various metal complexes (Cu, Pd, Mo) which are used for oxidation of sulfides and oxidative coupling of thiols [22], Mannich reaction [23], and Suzuki coupling reactions [24]. Also, in 2015, Rostamnia et al. [25] have reported the successful synthesis of water-dispersed magnetic nanoparticles (H_2O-DMNPs) of β-cyclodextrin modified Fe_3O_4 and their catalytic application in Kabachnik–Fields multicomponent reaction. Subsequently in 2017, Heidarizadeh et al. [26] have reported the immobilization of an enzyme (lipase) to Fe_3O_4/GO nanocomposite, and in 2018, Rakhtshah et al. [27] have reported copper Schiff base complex immobilized on silica-coated magnetic nanoparticles as catalyst for the synthesis of polysubstituted pyrroles.

Suzuki–Miyaura and Heck–Mizoroki cross-coupling reactions are versatile and important methods for C–C bond formation in organic synthesis. These reactions have many applications in industrial processes such as the synthesis of natural products, organic building blocks, biologically active compounds, pharmaceuticals, and agricultural derivatives [28–32]. The Suzuki and Heck C–C cross-coupling reactions catalyzed by palladium catalyst in the presence of phosphine auxiliary ligands. However, there are several problems in usage of palladium–phosphine systems like separation, recovery, and catalyst instability at high temperatures; moreover, phosphine ligands are toxic, expensive, and sensitive to air, which also limit their use in large-scale industrial application [33–36]. Therefore, the development of new heterogeneous phosphorus-free catalysts for the reactions under mild conditions is of immense interest, and there are reports of C–C coupling reactions with several heterogeneous catalysts [37–40]. In continuation of our research [41–43], herein, we report the preparation of novel, efficient, and green Fe_3O_4–Schiff base–Pd complex as catalyst (Scheme 1), and its high catalytic activity in carbon–carbon bond formation reactions. Moreover, the catalyst separation is done easily by an external magnet and the nanocatalyst can be reused for several times without significant degradation in activity.

Experimental

Preparation of the Fe_3O_4 magnetic nanoparticles (MNPs)

The mixture of $FeCl_3{\cdot}6H_2O$ (5.838 g, 0.0216 mol) and $FeCl_2{\cdot}4H_2O$ (2.147 g, 0.0108 mol) was dissolved in 100 mL deionized water at 80 °C under N_2 atmosphere and vigorous mechanical stirring conditions, until the salts dissolved completely. Then, 10 mL of 25% NH_4OH was added quickly into the reaction mixture and stirring was continued for 30 min. After 30 min, the reaction mixture was cooled to room temperature, and the black precipitate obtained was magnetically separated and washed several times by distilled water. Finally, the 2.5 g of the magnetic nanoparticles (MNPs) recovered.

Preparation of MNPs coated by 3-amino propyl triethoxy silane (Fe_3O_4–NH_2)

The obtained magnetic nanoparticles (MNPs) powder (1.5 g) was dispersed in 250 mL solution of ethanol and water (volume ratio, 1:1) by sonication for 30 min. Then, 3 mL of 3-aminopropyltriethoxysilane was added to the reaction mixture at 33–38 °C under N_2 atmosphere and mechanical stirring conditions for 8 h. The resulting product was separated by an external magnet and washed thoroughly with dry ethanol and dried under vacuum at room temperature that the 1.65 g of the amino-functionalized MNPs (Fe_3O_4–NH_2) obtained.

Preparation of Fe_3O_4 functionalized ninhydrin–Schiff base (Fe_3O_4–Schiff base)

The amino-functionalized MNPs (1 g) were dispersed in dry ethanol (10 mL) by ultrasonic bath for 20 min. Subsequently, ninhydrin (0.534 g, 3 mmol) and 0.5 mL acetic acid were added, and the mixture was refluxed for 24 h under N_2 atmosphere. Then, the reaction mixture was cooled, the precipitate was separated by magnetic decantation, washed several times by dry ethanol to remove the unattached substrates. The 1.2 g of the nanoparticles product (Fe_3O_4–Schiff base) was dried at room temperature.

Preparation of Fe_3O_4–Schiff base–Pd catalyst

The Fe_3O_4–Schiff base (1 g) were dispersed in 20 mL dry ethanol, and solution by ultrasonic bath for 20 min, and then $Pd(OAc)_2$ (0.5 g) was added reaction mixture. The resulting mixture was refluxed for 20 h under nitrogen atmosphere. Subsequently, excess of 0.203 g (1.2 mol) $NaBH_4$ were added to the reaction mixture for the reduction of Pd particles, and the reaction mixture was refluxed for 2 h under N_2 atmosphere. After that, the final product was magnetically separated and washed with copious amounts of dry ethanol and dried at room temperature and the 1.15 g of the Fe_3O_4–Schiff base–Pd catalyst obtained.

Scheme 1 Synthesis of Fe_3O_4–Schiff base–Pd

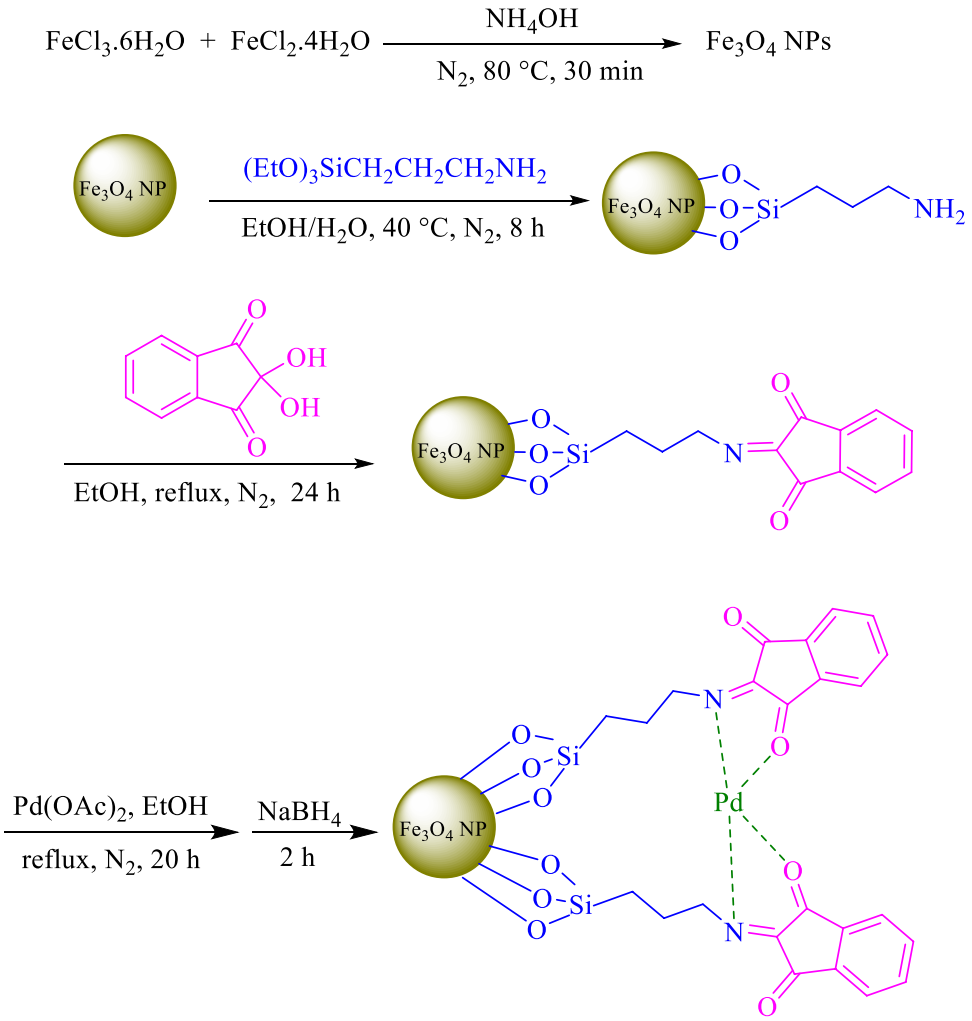

General procedure for the Suzuki reaction

The Fe_3O_4–Schiff base–Pd (0.91 mol%) was added to mixture of aryl halides (1 mmol), phenylboronic acid (1 mmol) and K_2CO_3 (3 mmol) in 2 mL of PEG-400 (polyethylene glycol) at 80 °C, and the mixture was stirred for the appropriate time. Completion of the reaction was indicated using TLC. After completion of the reaction, the catalyst was separated with an external magnet, then product was extracted with 10 mL of H_2O and ethyl acetate (3 × 10 mL). The organic layer was dried over Na_2SO_4. Then, the solvent was evaporated, and corresponding biphenyl was obtained in good to high yield.

General procedure for the Heck reaction

A mixture of aryl halides (1 mmol), *n*-butyl acrylate (or acrylonitrile) (1.2 mmol), K_2CO_3 (1.5 mmol) (base for acrylonitrile Na_2CO_3 3 mmol), 2 mL of PEG-400 (polyethylene glycol) and Fe_3O_4–Schiff base–Pd catalyst (1.46 mol%) was stirred at 120 °C temperature for an appropriate time. The progress of the reaction was monitored using TLC. After completion of the reaction, the reaction mixture was cooled to room temperature. The catalyst was separated using a magnet, then mixture was diluted with 10 mL of H_2O and extracted with diethyl ether (3 × 10 mL) and the organic layer was dried over anhydrous Na_2SO_4. Then, the solvent was evaporated, and the desired products was obtained.

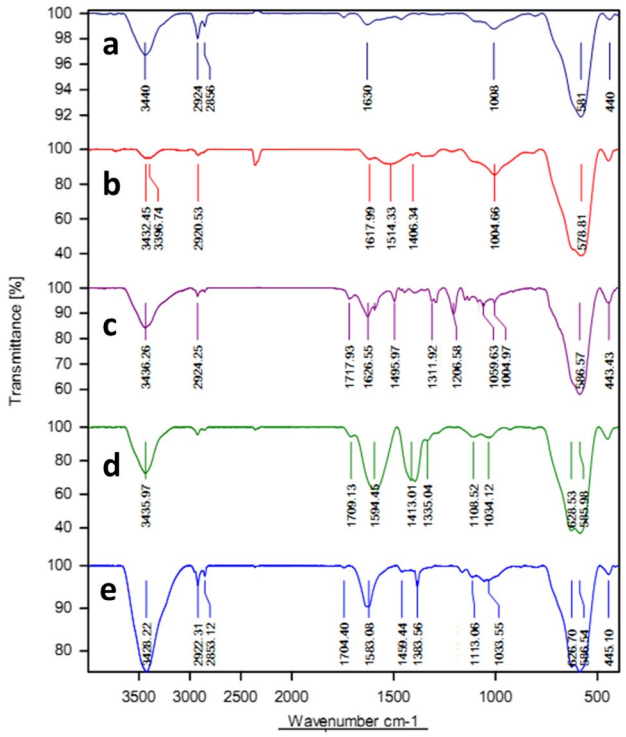

Fig. 1 FT-IR spectra of Fe_3O_4 (MNPs) (a), Fe_3O_4–NH_2 (b), Fe_3O_4–Schiff base (c), Fe_3O_4–Schiff base–Pd (d), reused Fe_3O_4–Schiff base–Pd (e)

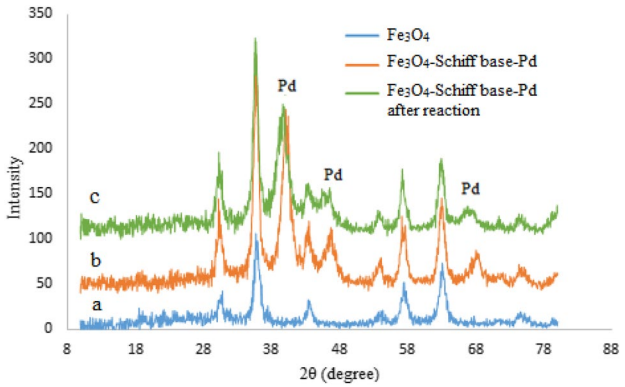

Fig. 2 XRD pattern of Fe_3O_4 (a), Fe_3O_4–Schiff base–Pd (b) and reused catalyst (c)

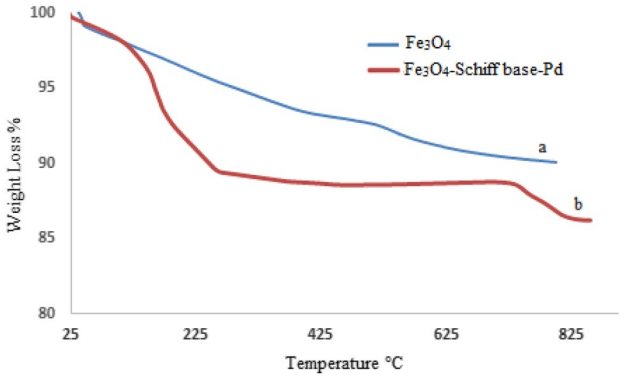

Fig. 3 TGA diagram of Fe_3O_4 (MNPs) (a), Fe_3O_4–Schiff base–Pd (b)

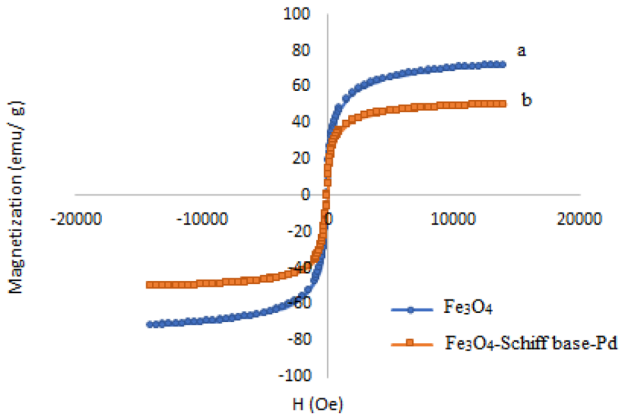

Fig. 4 VSM curve of Fe_3O_4 nanoparticles (a), Fe_3O_4–Schiff base–Pd (b)

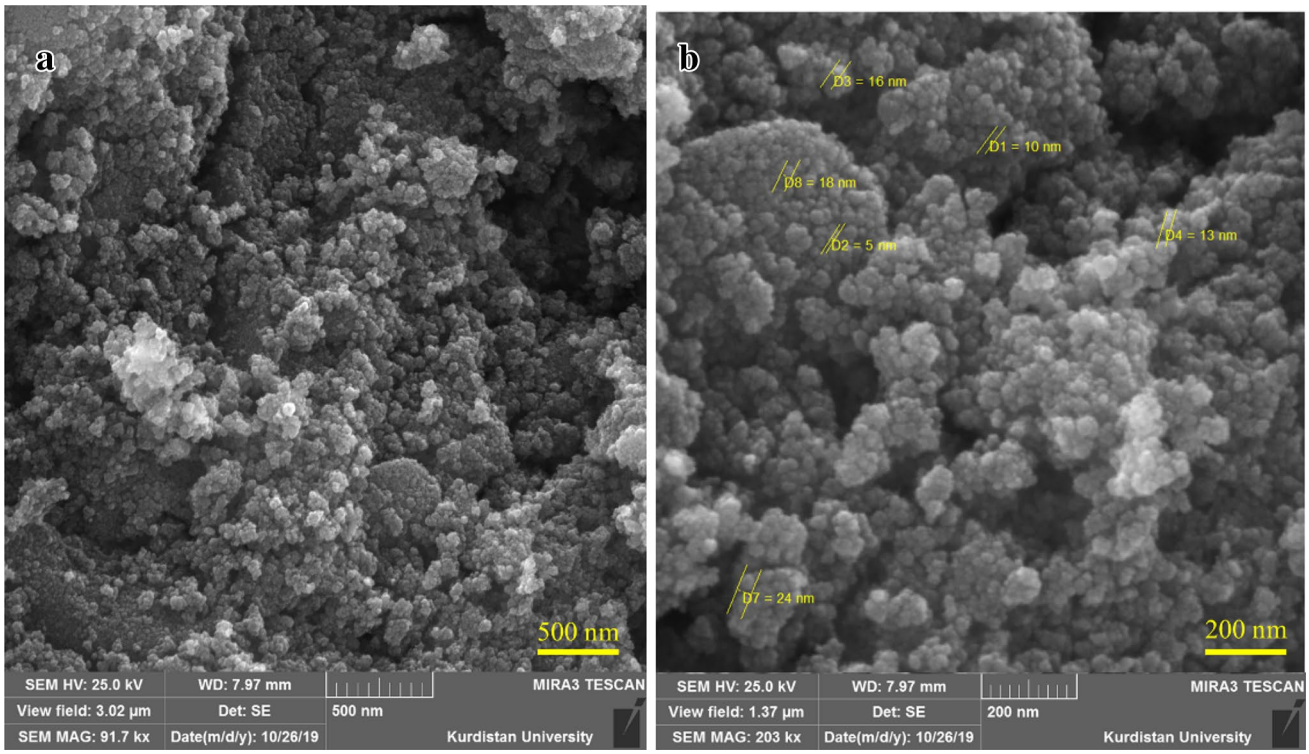

Fig. 5 SEM images of Fe_3O_4–Schiff base–Pd at 500 nm (a) and 200 nm (b)

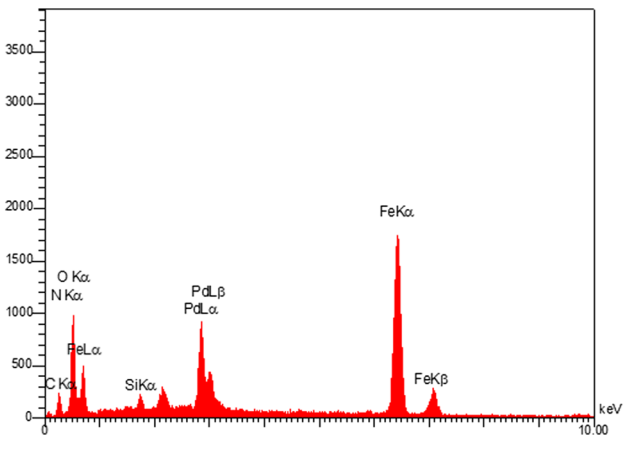

Fig. 6 EDS spectrum of Fe_3O_4–Schiff base–Pd

Results and discussions

Scheme 1 was shown the detail synthetic procedure for the preparation of Fe_3O_4–Schiff base–Pd as novel magnetic nanoparticle catalyst. The procedure for the synthesis of Fe_3O_4 nanoparticle is presented in the literature [42]. In the next step, the 3-amino propyl triethoxy silane (APTES) supported on Fe_3O_4 nanoparticle (Fe_3O_4–NH_2) was synthesized according to the reported procedure [44], and then, Fe_3O_4–Schiff base could also be obtained by the reaction of amine groups of APTES supported on Fe_3O_4 nanoparticles and ninhydrin ligand. Finally, the supported magnetic nanocatalyst Fe_3O_4–Schiff base–Pd was prepared via reaction of palladium(II) acetate and Fe_3O_4–Schiff base. Eventually, the supported magnetic nanocatalyst was obtained and characterized by different techniques such as FT-IR, XRD, TGA, ICP, VSM, SEM, and EDX-MAP.

Catalyst characterization

The catalyst has been characterized by Fourier transform infrared spectroscopy (FT-IR, Bruker, Germany), X-ray diffraction (XRD, GBC-Difftech MMA), thermogravimetric analysis (TGA, PerkinElmer Pyris Diamond, UK), inductively coupled plasma atomic emission spectrometry (ICP-OES, Optima 8000, PerkinElemr), vibrating sample magnetometer (VSM, MDKFD), scanning electron microscopy (SEM, FESEM-TESCAN MIRA3), and energy dispersive X-ray spectroscopy (EDS, FESEM-TESCAN MIRA3).

FT-IR spectrum for the samples of Fe_3O_4 MNPs (a), Fe_3O_4 nanoparticle functionalized with APTES (Fe_3O_4–NH_2) (b), Fe_3O_4–Schiff base (c) and Fe_3O_4–Schiff base–Pd catalyst (d) is shown in Fig. 1. The FT-IR spectrum for the MNPs (a) shows a stretching vibration of –OH group at about 3440 cm^{-1}, which are attached to the surface iron atoms. The strong absorption at 581 cm^{-1} is the characteristic of the

Table 1 Optimization of different parameters for the Suzuki reaction of iodobenzene with phenyl boronic acid in the presence of Fe_3O_4–Schiff base–Pd

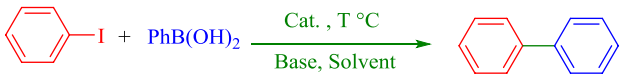

Entry	Solvent	Base	Temp (°C)	Cat. (mol%)	Time (min)	Yield[a] (%)
1	**PEG**	**K_2CO_3**	**60**	**0.91**	**20**	**98**
2	H_2O	K_2CO_3	60	0.91	15	95
3	EtOH	K_2CO_3	60	0.91	20	75
4	DMSO	K_2CO_3	60	0.91	20	64
5	DMF	K_2CO_3	60	0.91	20	52
6	PEG	–	60	0.91	300	–
7	PEG	Et_3N	60	0.91	20	50
8	PEG	Na_2CO_3	60	0.91	20	63
9	PEG	EtONa	60	0.91	20	50
10	PEG	KOH	60	0.91	20	20
11	PEG	$K_2CO_3^b$	60	0.91	20	64
12	PEG	K_2CO_3	40	0.91	20	38
13	PEG	K_2CO_3	80	0.91	15	95
14	PEG	K_2CO_3	60	–	1440	–
15	PEG	K_2CO_3	60	0.18	20	55
16	PEG	K_2CO_3	60	0.54	20	76
17	PEG	K_2CO_3	60	1.28	20	98

Reaction condition: iodobenzene (1 mmol), phenyl boronic acid (1 mmol), base (3 mmol), and solvent (2 mL)

Bold indicates opimized condition

[a]Isolated yield

[b]$K_2CO_3 = 1.5$ mmol

Fe–O stretching vibration, which demonstrates the existence of Fe_3O_4 components. In the FT-IR spectrum of Fe_3O_4–NH_2 (b), the existence of the anchored 3-aminopropyl triethoxy silane (APTES) is confirmed by stretching vibration of aliphatic C–H group that appear at 2920 cm^{-1}, and also a broad band appears at 3396–3432 cm^{-1} and 1004 cm^{-1}, which is related to the N–H and Si–O stretching vibrations, respectively. A new band observed in FT-IR spectrum of Fe_3O_4–Schiff base (c) at 1717 cm^{-1} can be attributed to the carbonyl bonds and the band observed at 1626 cm^{-1} could be assigned to the C=N stretching vibrations. These bands are evidence that ninhydrin has been successfully attached with terminal amine in Fe_3O_4–NH_2 and also confirm to the formation of Fe_3O_4–Schiff base. In the FT-IR of catalyst (d), the C=N bond shifted to a lower wave number and appear at 1594 cm^{-1}, which indicate the formation of Pd Schiff base complexes. The spectrum of the recovered Fe_3O_4–Schiff base–Pd (e) shows that the catalyst is stable during the reaction.

Crystal structure of synthesized nanocatalysts was investigated by X-ray powder diffraction analysis (XRD) (Fig. 2). The XRD pattern shows the characteristic peaks of bare Fe_3O_4 at $2\theta = 30.3°$, 35.7°, 43.3°, 53.7°, 57.3°, and 62.9° corresponding to the reflections of (2 2 0), (3 1 1), (4 0 0), (4 2 2), (5 1 1), and (4 4 0). The XRD pattern of Fe_3O_4–Schiff base–Pd catalyst matches well with the characteristic peaks of bare Fe_3O_4, which indicates retention of the crystalline spinel ferrite core structure during functionalization of MNPs. The new peaks appeared at $2\theta = 39.8$, 47.6 and 67.4 which attributed to the Pd species. The XRD diagram of reused catalysts shows that the structure of catalyst is stable during the reaction.

The thermogravimetric analysis (TGA) was used to determine the thermal stability and percentage of chemisorbed organic functional groups on the surface of the magnetic nanoparticles. The TGA curve of the bare Fe_3O_4 nanoparticles (a) and Fe_3O_4–Schiff base–Pd (b) shows the mass loss of the organic groups as it decomposes upon heating (Fig. 3). The weight loss about 4% in the TGA curve of Fe_3O_4, at temperatures below 200 °C is assigned to the removal of physically adsorbed organic solvents and surface –OH groups (Fig. 3a). Moreover, the weight loss occurs about 5% in the temperature range between 250 and 630 °C may be due to the thermal crystal phase transformation from Fe_3O_4

Table 2 Suzuki coupling of various aryl halides with phenyl boronic acid catalyzed by Fe_3O_4–Schiff base–Pd catalyst

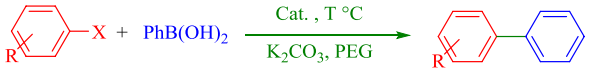

Entry	Aryl halide	Time (min)	Yield (%)[a]	TOF (h^{-1})	MP (°C) [Ref.]
1	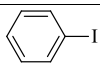	20	98	324.5	66–68 [46]
2	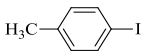	70	93	87.6	44–46 [47]
3		90	91	66.3	Oil [48]
4	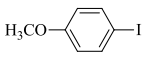	80	97	79.7	84–86 [49]
5	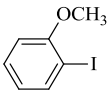	60	96	104.9	Oil [50]
8	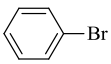	30	91	198.9	66–68 [46]
9	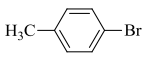	80	95	78	44–46 [47]
10	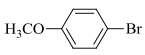	165	93	36.9	84–86 [49]
11	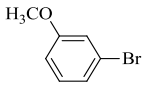	75	98	85.6	Oil [51]
12	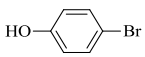	35	99	186.5	156–159 [52]
13	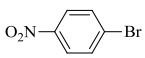	50	98	129	112–114 [51]
14	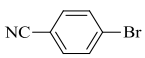	55	98	116.9	83–86 [52]
15	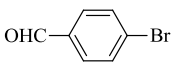	60	90	98.3	56–58 [53]
16	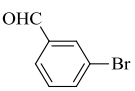	75	92	80.4	48–50 [50]
17	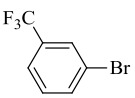	30	88	192.3	Viscous liquid [54]
18	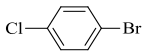	40	96	158.9	70–72 [55]
19	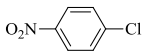	120	67[b]	36.61	112–114 [51]

Table 2 (continued)

Reaction condition: aryl halides (1 mmol), phenyl boronic acid (1 mmol), K_2CO_3 (3 mmol), Fe_3O_4–Schiff base–Pd (0.91 mol%) in 2 mL of PEG and at 60 °C

[a]Isolated yield

[b]Fe_3O_4–Schiff base–Pd (1.83 mol%) in 2 mL of PEG and at 80 °C

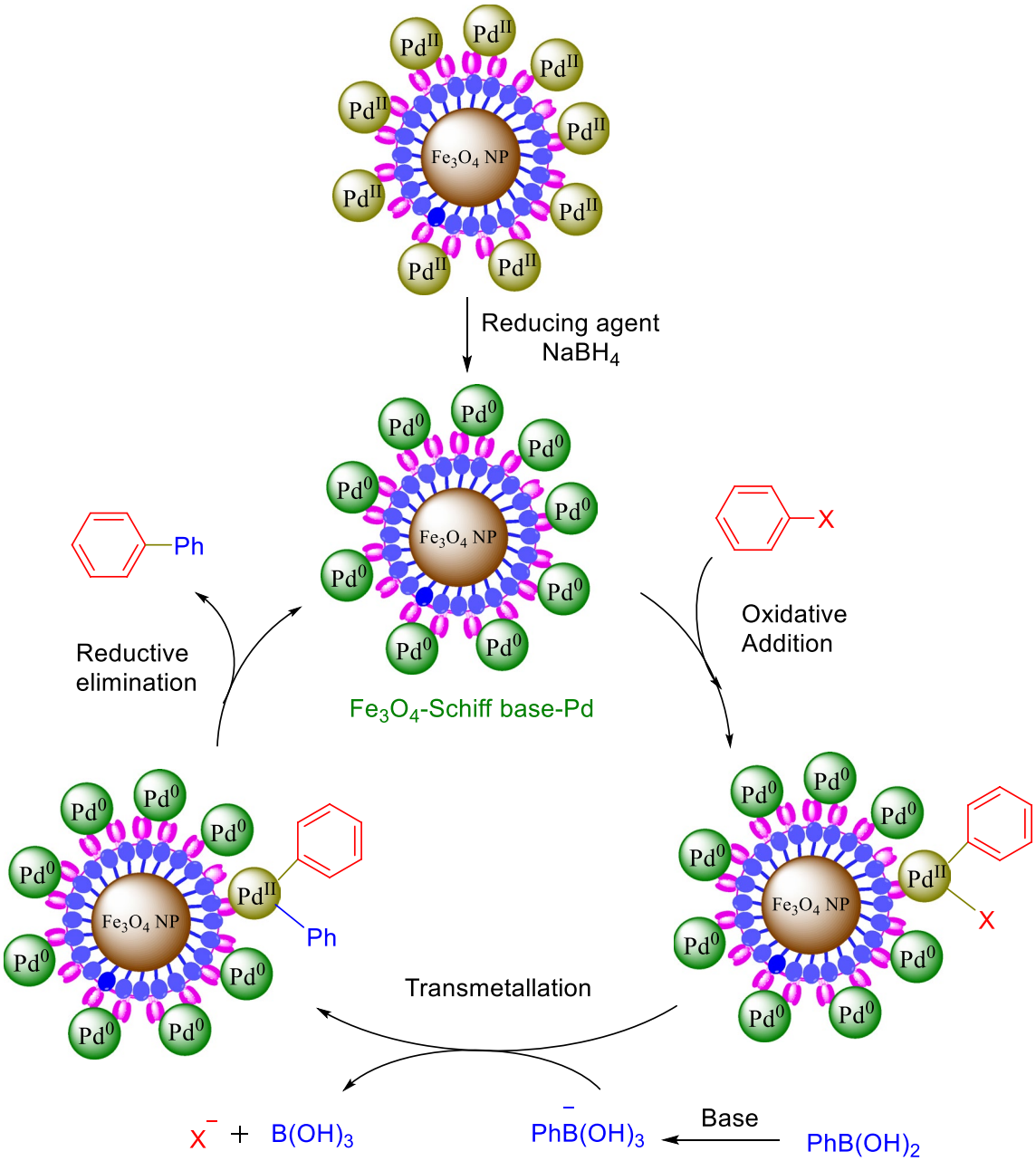

Scheme 2 Mechanism of the Fe_3O_4–Schiff base–Pd catalyzed Suzuki reaction

to γ-Fe_2O_3 [45]. There are three weight loss steps in the TGA curve of Fe_3O_4–Schiff base–Pd (Fig. 3b). Firstly, indicates a weight loss at about 5% below 200 °C which is owing to the removal of water molecules from the catalyst surface. The steps two and three of weight losses at 200–800 °C may correspond to the degradation of 3-(aminopropyl) triethoxysilane groups and organic ligands in the Schiff base–Pd complex.

The magnetic property of Fe_3O_4 nanoparticles and Fe_3O_4–Schiff base–Pd recorded at room temperature using a vibrating sample magnetometer (VSM) technique (Fig. 4). The magnetic measurement shows that the

Table 3 Optimization of different parameters for the Heck reaction of iodobenzene with *n*-butyl acrylate in the presence of Fe_3O_4–Schiff base–Pd

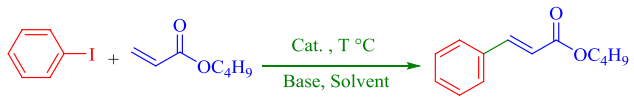

Entry	Solvent	Base	Temp (°C)	Cat. (mol%)	Time (min)	Yield[a] (%)
1	**PEG**	**K_2CO_3**	**120**	**1.46**	**10**	**98**
2	H_2O	K_2CO_3	120	1.46	10	25
3	EtOH	K_2CO_3	120	1.46	10	20
4	DMSO	K_2CO_3	120	1.46	10	78
5	DMF	K_2CO_3	120	1.46	10	83
6	PEG	–	120	1.46	300	–
7	PEG	Et_3N	120	1.46	10	87
8	PEG	Na_2CO_3	120	1.46	10	75
9	PEG	EtONa	120	1.46	10	40
10	PEG	$NaHSO_4$	120	1.46	10	20
11	PEG	K_2CO_3[b]	120	1.46	10	95
12	PEG	K_2CO_3	80	1.46	10	50
13	PEG	K_2CO_3	100	1.46	10	90
14	PEG	K_2CO_3	120	–	1440	–
15	PEG	K_2CO_3	120	0.73	10	88
16	PEG	K_2CO_3	120	1	10	90
17	PEG	K_2CO_3	120	1.83	10	98

Reaction condition: aryl halides (1 mmol), *n*-butyl acrylate (1.2 mmol), base (1.5 mmol), and solvent (2 mL)

Bold indicates opimized condition

[a]Isolated yield

[b]$K_2CO_3 = 3$ mmol

Fe_3O_4–Schiff base–Pd has a saturated magnetization value of 49.9 emu g^{-1}. The VSM curve of the Fe_3O_4 nanoparticle is 71 emu g^{-1} which has higher magnetic value in comparison with synthesized nanocatalyst. Decrease in magnetic property of Fe_3O_4–Schiff base–Pd is due to the coating of silica and the attached of organic layers on Fe_3O_4 nanoparticles.

The morphology and nanoparticle size of the catalyst was characterized by scanning electron microscopy. The SEM images of the Fe_3O_4–Schiff base–Pd nanocatalyst at different magnifications are shown in Fig. 5. According to Fig. 5, the surface morphology of the catalyst shows uniform and spherical particles with size of less than 24 nm.

The energy dispersive X-ray spectroscopy (EDS) spectrum shows the presence of various elements in the catalyst (Fig. 6).

The amount loading of Pd on the Fe_3O_4–Schiff base, determined by inductively coupled plasma atomic emission spectrometry (ICP-AES). The ICP analysis showed amount of Pd in catalyst was 1.88×10^{-3} mol g^{-1}. Also analysis of the recovered catalyst by the ICP technique was 1.80×10^{-3} mol g^{-1} indicates that the leaching of the Pd metal was negligible and about 0.72%.

Catalytic study

After preparation of Fe_3O_4–Schiff base–Pd, its catalytic activities were evaluated for C–C bond forming reactions such as the Suzuki–Miyaura and Mizoroki–Heck coupling reaction. For this purpose, the Suzuki coupling reaction of iodobenzene with phenyl boronic acid was chosen as a simple model reaction to optimize the reaction conditions, including catalyst amount, solvent, base and effect of temperature (Table 1). Initially, different solvents such as H_2O, dimethylformamide (DMF), dimethylsulfoxide (DMSO), polyethylene glycol (PEG-400), and ethanol were examined (entries 1–5) in the presence of 0.91 mol% of Fe_3O_4–Schiff base–Pd. In both PEG (98%) and water (95%) (entries 1 and 2), high yields of the product were observed, but trace amounts of products were obtained in Suzuki reaction of the various aryl halides with phenyl boronic acid in water; thus, PEG was as the best solvent for this reaction. To investigate the effect of bases in the model reaction, various bases such as K_2CO_3, Na_2CO_3, EtONa, Et_3N, and KOH were examined (entries 7–10). In the case of K_2CO_3, the catalyst was very

Table 4 Heck coupling of various aryl halides with *n*-butyl acrylate or acrylonitrile catalyzed by Fe_3O_4–Schiff base–Pd catalyst

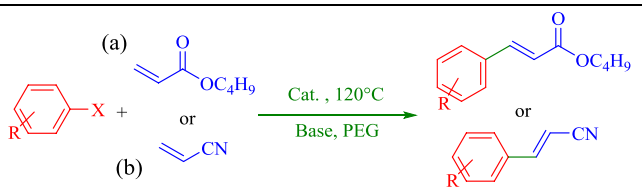

Entry	Aryl halide	Reagent	Time (min)	Yield (%)[a]	TOF (h^{-1})	MP (°C) [Ref.]
1	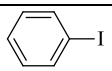	a	10	98	419.5	Oil [57]
2	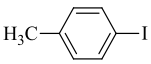	a	15	98	268.4	Oil [55]
3	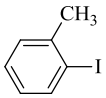	a	30	99	135.6	Oil [55]
4	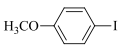	a	30	92	126	Oil [55]
5	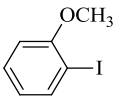	a	60	95	65	Oil [55]
6	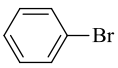	a	30	88	120.5	Oil [57]
7	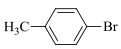	a	60	90	61.6	Oil [55]
8	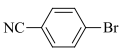	a	80	90	46.3	40–42 [58]
9	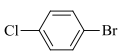	a	135	98	29.8	Oil [58]
10	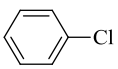	a	270	88[b]	13.3	Oil [57]
11	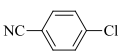	a	285	80[b]	11.5	40–42 [58]
12	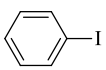	b	50	92	74.2	Oil [59]
13	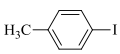	b	180	90	20.5	Oil [60]
14	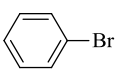	b	105	83	32.4	Oil [59]
15	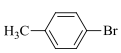	b	300	80	10.9	Oil [60]

Table 4 (continued)

Reaction condition reagent (a): aryl halides (1 mmol), *n*-butyl acrylate (1.2 mmol), K_2CO_3 (1.5 mmol), Fe_3O_4–Schiff base–Pd (1.46 mol%) in 2 mL of PEG and at 120 °C. Reaction condition reagent (b): aryl halides (1 mmol), acrylonitrile (1.2 mmol), Na_2CO_3 (3 mmol), Fe_3O_4–Schiff base–Pd (1.46 mol%) in 2 mL of PEG and at 120 °C

[a]Isolated yield

[b]Reaction condition: aryl halides (1 mmol), *n*-butyl acrylate (1.2 mmol), K_2CO_3 (3 mmol), Fe_3O_4–Schiff base–Pd (2.1 mol%) in 2 mL of PEG and at 120 °C

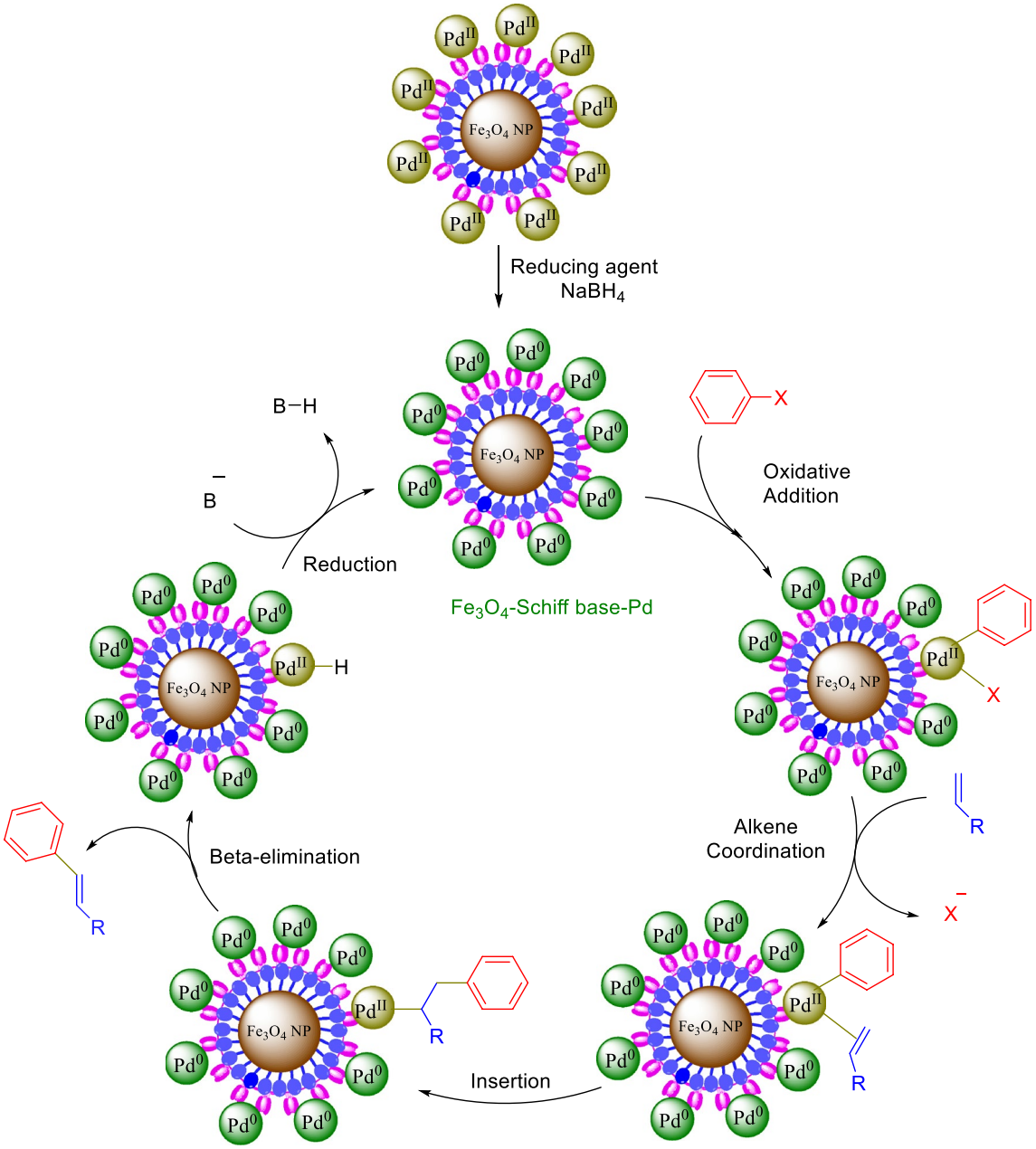

Scheme 3 Mechanism of the Fe_3O_4–Schiff base–Pd catalyzed Heck reaction

active and best yield of product obtained for the reaction (entry 1), when the amount of K_2CO_3 from 3 to 1.5 mmol was decreased, lower yield is obtained (entry 11). In the next step, this model reaction by different temperatures including 40, 60, and 80 °C was examined, and the best results were obtained in temperature of 60 °C. Increasing the temperature to 80 °C, did not effectively increase the yield of product (entry 13).

Finally, to optimize the catalyst amount, different quantities of catalyst were evaluated in the model reaction. As shown in Table 1, for the coupling reaction in the absence of catalyst, no formation of product occurs after 24 h (entry 14), but experiments showed that 0.91 mol% of catalyst are the sufficient amount for the completion of the reaction. Using more of catalyst did not effectively increase on the yield or decrease time of the reaction (entry 17). With the optimized reaction conditions, the generality and scope of the catalytic utility of Fe_3O_4–Schiff base–Pd catalyst in Suzuki reaction was demonstrated with a range of aryl halides (chlorides, bromides and iodides) and phenyl boronic acid (Table 2). The biphenyl derivatives were obtained in satisfactory yields and the results are summarized in Table 2. However, the results of the Suzuki coupling reactions depend on the type of halide element, the positions of the substitution groups on aromatic ring and the effect of various electron donating and electron withdrawing groups. The catalyst high activity and excellent yield of products were obtained in reaction of aryl iodides and bromides with phenyl boronic acid.

The suggested mechanism for Suzuki reaction in the presence of Fe_3O_4–Schiff base–Pd catalyst is outlined in Scheme 2 [56].

In the second part of our organic program, the application of Fe_3O_4–Schiff base–Pd catalyst was examined in the Heck cross-coupling reaction of aryl halides and olefins in the presence of a base. For finding the optimal reaction conditions, the Heck reaction of iodobenzene with *n*-butyl acrylate was chosen as a model reaction, and various parameters such as catalyst amount, kind of solvent, effects of bases and temperature were investigated for the model reaction (Table 3). Initially, different solvents including H_2O, EtOH, DMF, DMSO and PEG-400 were examined and the best results for the Heck reaction were obtained in PEG (entry 1). Also, the effects of different bases were examined. The highest yield in the shortest reaction time was achieved using 1.5 mmol of K_2CO_3. While use of Na_2CO_3 and Et_3N give moderate yields and in the presence of other bases, EtONa and $NaHSO_4$ low-to-moderate yields of product are obtained (entries 7–10). The use of 3 mmol amount of K_2CO_3 does not effectively increase on the yield and time of the reaction (entry 11). Evaluation of the model reaction under different temperatures such as 80, 100, and 120 °C has shown that greatest yield was obtained at 120 °C (entries 12–13). In addition, different amounts of catalyst were investigated for this reaction, and 1.46 mol% of catalyst was found to optimal amount (entries 15–17). The higher amounts of catalyst, the desired product was obtained in an almost similar yield. After the optimized reaction conditions, to investigate the scope of the catalytic system in Heck reaction, the coupling of various aryl halides with *n*-butyl acrylate was examined and the results are shown in Table 4.

The results demonstrated that the Fe_3O_4–Schiff base–Pd catalyst was effective for the couplings of the aryl halides with both electron withdrawing and donating groups with butyl acrylates. To extend the scope of our work, we next examined the coupling of various aryl halides with acrylonitrile (1.2 mmol), in the presence of 1.46 mol% of catalyst, PEG and 3 mmol of Na_2CO_3 as base at 120 °C. The results are summarized in Table 4. In the Heck reaction, the reaction time of aryl iodides and aryl bromides were less than aryl chlorides.

The proposed mechanism for Heck reaction in the presence of Fe3O4–Schiff base–Pd catalyst was outlined in Scheme 3 [56].

Recyclability of the catalyst

The recycling of the heterogeneous catalysts is an important advantage for commercial applications. To investigate this issue, the recovery and reusability of the catalyst was examined for a Suzuki reaction of iodobenzene and phenyl boronic acid, and a Heck reaction of iodobenzene and *n*-butyl acrylate as model reactions under the optimized conditions. After the completion of reaction, the catalyst was simply separated from the reaction mixture using an external magnet and washed with water and ethanol to remove of organic residuals, dried and reused for next runs. As shown in Fig. 7, the catalyst can be recovered for six runs without any significant loss in its catalytic activity and performance.

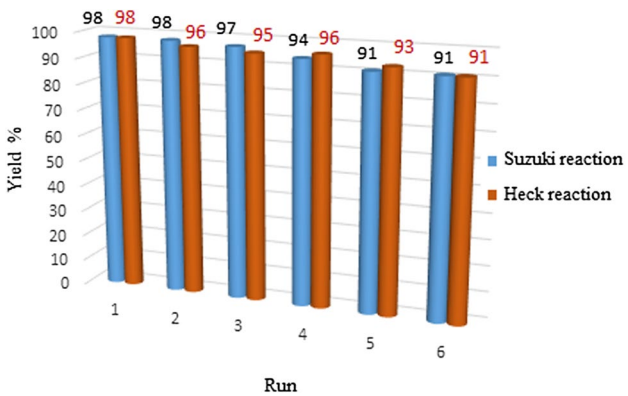

Fig. 7 Recyclability of Fe_3O_4–Schiff base–Pd in the Suzuki–Miyaura and Heck–Mizoroki model reaction

Table 5 Comparison results of Fe_3O_4–Schiff base–Pd with other catalysts for the coupling of iodobenzene with phenylboronic acid

Entry	Catalyst	Condition	Time (min)	Yield (%)	TOF (h^{-1})	References
1	Pd(II)–NHC complex (0.01 mmol)	DMA, Cs_2CO_3, 100 °C	24 h	99	4.1	[57]
2	*N*,*N*′-bis(2-pyridinecarboxamide)-1,2-benzene palladium complex (1 mol%)	H_2O, K_2CO_3, 100 °C	180	97	32.3	[61]
3	Pd/TiO_2 (0.7 mol%)	NMP:H_2O, Na_2CO_3, 120 °C, N_2	240	97	34.6	[62]
4	PdeSchiff base@MWCNTs (0.1 mol%)	K_2CO_3, DMF/H_2O (v/v ¼ 1:1), 60 °C	120	99	495	[63]
5	Pd@SBA-15/ILDABCO (0.5 mol%)	K_2CO_3, H_2O, 80 °C	90	97	129	[64]
6	Pd-TEDETA-MCM-41 (0.57 mol%)	H_2O, Na_2CO_3, 60 °C, r.t	70	92	138.3	[41]
7	$(ZrO)_2Fe_2O_5$	KOH, DMSO, 110 °C	900	83	5.17	[37]
8	HMS–CPTMS–Cy–Pd (0.008 g)	K_2CO_3, PEG, 100 °C	15	95	292	[42]
9	Pd(0)-Arg-boehmite (8 mg, 1.08 mol%)	Na_2CO_3, PEG, 80 °C	45	98	121	[56]
10	Fe_3O_4–Schiff base–Pd (0.91 mol%)	K_2CO_3, PEG, 60 °C	20	98	324.5	This work

Hot filtration test

Also hot filtration test was examined to discard the possibility of palladium leaching. In this light, we studied a hot filtration technique for the Suzuki coupling of 4-boromobenzonitrile with phenylboronic acid. This reaction carried out at 55 min and yield of product was 98%. We repeated the reaction and yield of product in half time of the reaction was 55%. In another same reaction after 25 min, catalyst was separated by an external magnet and washed with hot ethanol, and then the solution was allowed to go for the remaining half stirring. After purification, yield of product was obtained 52%. This test indicates that the leaching of the Pd metal was negligible.

Comparison of the catalyst

In order to investigate the catalytic activity of Fe_3O_4–Schiff base–Pd, we compared the results of the coupling of iodobenzene with phenylboronic acid (Table 5) with the previously reported catalysts in the literature and results are given in Table 5. Overall, the obtained catalyst showed better yield and higher TOF values in shorter reaction time than other catalysts reported in the previous literatures. Also, this catalyst is comparable in terms non-toxicity, simple and inexpensive procedure, stability, and easy separation of the catalyst. Moreover, the recovery and recyclability of this catalyst is faster and easier than the other catalysts.

Conclusion

In summary, Fe_3O_4–Schiff base–Pd complex can be used as a novel, green, efficient, and reusable nanocatalyst for Suzuki–Miyaura and Heck–Mizoroki reactions. This catalyst offers several advantages including high catalytic activity, excellent yields, short reaction time, and mild reaction conditions. Furthermore, the catalyst could be simply recovered from the reaction mixture using an external magnet and reused up to 6 times without a significant loss in activity.

Acknowledgements This work was supported by the research facilities of Ilam University, Ilam, Iran.

References

1. H. Nur, Sh Ikeda, B. Ohtani, J. Catal. **204**, 402–408 (2001)
2. V. Polshettiwar, R. Luque, A. Fihri, H. Zhv, M. Bouhrara, J.-M. Basset, Chem. Rev. **111**, 3036–3075 (2011)
3. S. Shylesh, V. Schunemann, W.R. Thiel, Angew. Chem. Int. Ed. **49**, 3428–3459 (2010)
4. Y. Zhu, L.P. Stubbs, F. Ho, R. Liu, C.P. Ship, J.A. Maguire, N.S. Hosmane, Chem. Cat. Chem. **2**, 365–374 (2010)
5. V. Pplshettiwar, R.S. Varma, Green Chem. **12**, 743–754 (2010)
6. R.K. Sharma, M.B. Gawande, Sh Sharma, S. Dutta, R. Zboril, Green Chem. **17**, 3207–3230 (2015)
7. M. Heitbaum, F. Glorius, I. Escher, Angew. Chem. Int. Ed. **45**, 4732–4762 (2006)
8. ChW Lim, I.S. Lee, Nano Today **5**, 412–434 (2010)
9. M. Nikoorazm, A. Ghorbani-Choghamarani, H. Mahdavi, S.M. Esmaeili, Microporous Mesoporous Mater. **211**, 174–181 (2015)
10. F. Tavakoli, M. Mamaghani, M. Sheykhan, Appl. Organometal. Chem. **33**, e5083 (2019)
11. K. Bahrami, M.M. Khodaei, P. Fattahpour, Catal. Sci. Technol. **1**, 389–393 (2011)
12. D. Saha, R. Sen, T. Maity, S. Koner, Langmuir **29**, 3140–3151 (2013)
13. A. Ghorbani-Choghamarani, P. Moradi, B. Tahmasbi, J. Iran. Chem. Soc. **16**, 511–521 (2019)
14. D.R. Paul, L.M. Robeson, Polymer **49**, 3187–3204 (2008)
15. M. Moghadam, H. Salavati, Z. Pahlevanneshan, J. Iran. Chem. Soc. **15**, 529–536 (2018)
16. T. Cheng, D. Zhang, H. Li, G. Liu, Green Chem. **16**, 3401–3427 (2014)
17. P.H. Li, B.K. Li, H.C. Hu, X.N. Zhao, Z.H. Zhang, Catal. Commun. **46**, 118–122 (2014)

18. X.N. Zhao, H.C. Hu, F.J. Zhang, Z.H. Zhang, Appl. Catal. A Gen. **482**, 258–265 (2014)
19. H. Hamadi, M. Kooti, M. Afshari, Z. Ghiasifar, N. Adibpour, J. Mol. Catal. A Chem. **373**, 25–29 (2013)
20. M.A. Zolfigol, A.R. Moosavi-Zare, P. Moosavi, V. Khakyzadeh, A. Zare, C. R. Chim. **16**, 962–966 (2013)
21. M. Afshari, M. Gorjizadeh, S. Nazari, M. Naseh, J. Magn. Magn. Mater. **363**, 13–17 (2014)
22. A. Ghorbani-Choghamarani, B. Ghasemi, Z. Safari, G. Azadi, Catal. Commun. **60**, 70–75 (2015)
23. D. Yuan, L. Chen, L. Yuan, Sh Liao, M. Yang, Q. Zhang, Chem. Eng. J. **287**, 241–251 (2016)
24. J. Rakhtshaha, B. Shaabania, S. Salehzadehb, N. Hosseinpour Moghadam, Bioorg. Chem. **85**, 420–430 (2019)
25. S. Rostamnia, E. Doustkhah, J. Mang. Mang. Mater. **386**, 111–116 (2015)
26. M. Heidarizadeh, E. Doustkhah, S. Rostamnia, P. Fathi Rezaei, F. Darvishi Harzevili, B. Zeynizadeh, Int. J. Biol. Macromol. **101**, 696–702 (2017)
27. J. Rakhtshah, B. Shaabani, S. Salehzadeh, N. Hosseinpour Moghadam, Appl. Organometal. Chem. **33**, e4754 (2018)
28. C. Diebold, S. Schweizer, J.-M. Becht, C.L. Drian, Org. Biomol. Chem. **8**, 4834–4836 (2010)
29. N. Salam, S.K. Kundu, A.S. Roy, P. Mondal, A. Bhaumik, S.M. Islam, Dalton Trans. **43**, 7057–7068 (2014)
30. K.A. Crawford, A.H. Cowley, S.M. Humphrey, Catal. Sci. Technol. **4**, 1456–1464 (2014)
31. H. Shen, C. Chen, C. Shen, A. Wang, P. Zhang, Catal. Sci. Technol. **5**, 2065–2071 (2015)
32. F.S. Han, Chem. Soc. Rev. **42**, 5270–5298 (2013)
33. H. Firouzabadi, N. Iranpoor, F. Kazemi, M. Gholinejad, J. Mol. Catal. A Chem. **357**, 154–161 (2012)
34. S. Sobhani, Z. Pakdin-Parizi, Appl. Catal. A Gen. **479**, 112–120 (2014)
35. Sh Gao, Y. Huang, M. Cao, T.F. Liu, R. Cao, J. Mater. Chem. **21**, 16467–16472 (2011)
36. Y.Y. Peng, J. Liu, X. Lei, Z. Yin, Green Chem. **12**, 1072–1075 (2010)
37. A. Ghorbani-Choghamarani, M. Mohammadi, Z. Taherinia, J. Iran. Chem. Soc. **16**, 411–421 (2019)
38. Sh Ann Babu, S. Saranya, K.R. Rohit, G. Anilkumar, Chem. Sel. **4**, 1019–1022 (2019)
39. M. Rajabzadeh, R. Khalifeh, H. Eshghi, M. Bakavoli, J. Catal. **360**, 261–269 (2018)
40. H. Wang, D. Sun, Q. Lu, F. Wang, L. Zhao, Z. Zhang, X. Wang, H. Liu, Nanoscale **11**, 5240–5246 (2019)
41. M. Hajjami, M. Cheraghi, Catal. Lett. **146**, 1099–1106 (2016)
42. M. Hajjami, F. Gholamian, RSC Adv. **6**, 87950–87960 (2016)
43. M. Hajjami, S. Kolivand, Appl. Organometal. Chem. **30**, 282–288 (2016)
44. A. Ghorbani-Choghamarani, B. Tahmasbi, N. Noori, R. Ghafouri-Nejad, J. Iran. Chem. Soc. **14**, 681–693 (2017)
45. A. Ghorbani-Choghamarani, Z. Darvishnejad, M. Norouzi, Appl. Organometal. Chem. **29**, 170–175 (2015)
46. S.D. Cho, H.K. Kim, H.S. Yim, M.R. Kim, J.K. Lee, J.J. Kim, Y.J. Yoon, Tetrahedron **63**, 1345–1352 (2007)
47. J. Masllorens, I. Gonzalez, A. Roglans, Eur. J. Org. Chem. **1**, 158–166 (2007)
48. P.D. Stevens, J. Fan, H.M.R. Gardimalla, M. Yen, Y. Gao, Org. Lett. **7**, 2085–2088 (2005)
49. B. Lü, C. Fu, S. Ma, Tetrahedron Lett. **51**, 1284–1286 (2010)
50. L. Emmanuvel, A. Sudalai, Arkivoc **14**, 126–133 (2007)
51. Y. Wang, J. Luo, Z. Liu, Appl. Organometal. Chem. **27**, 601–605 (2013)
52. L. Bai, J.X. Wang, Adv. Synth. Catal. **350**, 315–320 (2007)
53. M. Samarasimhareddy, G. Prabhu, T.M. Vishwanatha, V.V. Sureshbabu, Synthesis **45**, 1201–1206 (2013)
54. N.S.C. Ramesh Kumar, I. Victor Paul Raj, A. Sudalai, J. Mol. Catal. A Chem. **269**, 218–224 (2007)
55. A. Naghipour, A. Fakhri, Catal. Commun. **73**, 39–45 (2016)
56. B. Tahmasbi, A. Ghorbani-Choghamarani, Catal. Lett. **147**, 649–662 (2017)
57. Q. Xu, W.L. Duan, Z.Y. Lei, Z.B. Zhu, M. Shi, Tetrahedron **61**, 11225–11229 (2005)
58. N. Iranpoor, H. Firouzabadi, A. Tarassoli, M. Fereidoonnezhad, Tetrahedron **66**, 2415–2421 (2010)
59. Y. Leng, F. Yang, K. Wei, Y. Wu, Tetrahedron **66**, 1244–1248 (2010)
60. A. Ghorbani-Choghamarani, B. Tahmasbi, P. Moradi, Appl. Organometal. Chem. **30**, 422–430 (2016)
61. M. Gholinejad, H.R. Shahsavari, Inorg. Chim. Acta **421**, 433–438 (2014)
62. M. Nasrollahzadeh, S.M. Sajadi, J. Colloid Interface Sci. **465**, 121–127 (2016)
63. M. Navidi, N. Rezaei, B. Movassagh, J. Organomet. Chem. **743**, 63–69 (2013)
64. S. Rostamnia, E. Doustkhah, B. Zeynizadeh, Microporous Mesoporous Mater. **222**, 87–93 (2016)

Affiliations

Maryam Hajjami[1] · Zeinab Shirvandi[1]

✉ Maryam Hajjami
mhajjami@yahoo.com; m.hejami@ilam.ac.ir

[1] Department of Chemistry, Faculty of Science, Ilam University, P.O. Box 69315516, Ilam, Iran